MADRID
inter.noise 2019
June 16 - 19
NOISE CONTROL FOR A BETTER ENVIRONMENT

On a relative shift in the periodic micro-geometry and other causes for discrepancy in the microstructure-based modelling of 3D-printed porous media

Zieliński, Tomasz G.[1]
Institute of Fundamental Technological Research of the Polish Academy of Sciences
ul. Pawinskiego 5B, 02-106 Warsaw, Poland

Červenka, Milan[2]
Czech Technical University in Prague, Faculty of Electrical Engineering
Technická 2, 166 27 Prague 6, Czech Republic

ABSTRACT

Samples with periodic microstructures, designed for good sound absorption, have been manufactured by 3D printing. Typically, however, the acoustical properties of the resulting samples differ from those predicted. Two causes of the discrepancies are (1) inaccuracies related to the 3D-printing resolution and (2) imperfections resulting from micro-fibres, micro-pores, and pore surface roughness, created during manufacture. Discrepancies due to the first cause can be addressed, post hoc, by updating the idealised periodic geometric model used for creating the codes for fabrication on the basis of a survey using a scanning microscope, or through computerised micro-tomography scans. Reducing the discrepancies due to the second cause requires a relatively significant further modelling effort. Another cause for small discrepancies is when two layers of the same periodic porous material and thickness differ only by a relative shift of the internal geometry of the periodic Representative Volume Element (RVE). This causes the absorption peaks to be shifted in frequency. A modelling procedure is proposed to take this into account.

Keywords: Sound absorption, Periodic porous media, Additive manufacturing
I-INCE Classification of Subject Number: 35
(see http://i-ince.org/files/data/classification.pdf)

[1]tzielins@ippt.pan.pl
[2]milan.cervenka@fel.cvut.cz

1. INTRODUCTION

Additive manufacturing technologies [1] have recently become a very convenient tool for fabrication of samples of novel acoustic materials (and meta-materials) with designed periodic micro-geometries, even though the resolution, accuracy and surface quality available to most of these technologies are still away from the required level. It has been observed that imperfections related to a particular technology and device used for fabrication lead to specific discrepancies with respect to the results of modelling done during the design process, see, e.g., [2, 3]. This work discusses some issues concerning designing, manufacturing and modelling of periodic sound absorbing materials (or samples of such materials), which are fabricated with such modern additive manufacturing technologies [1]. In particular, an effect of a relative shift in the periodicity of samples of the same periodic porous material is studied with respect to change in the sound absorption. For the purpose of this paper, a simple periodic design is proposed and used to manufacture two porous samples. The samples are measured in the impedance tube for sound absorption [4] and the (updated) periodic design is used for modelling to calculate predictions. The modelling involves Direct Numerical Simulations (DNS) based on the linearised and harmonic, fully-coupled (i.e., compressible) Navier-Stokes equations, as well as the dual-scale approach with microstructural analyses done on a Periodic Unit Cell (PUC) and macroscopic analyses of wave propagation using the Helmholtz equation of linear acoustics and the Johnson-Champoux-Allard-Pride-Lafarge (JCAPL) model [5] for porous media. For the hybrid dual-scale modelling see, e.g., [6–15].

2. MICRO- AND MACRO-GEOMETRY OF THE ANALYSED PROBLEM

2.1. Panels with periodic porosity

Figure 1 shows cross-sectional views of two porous panels backed with an air cavity with depth ℓ_a. In each case, the panels have the same thickness ℓ_p and (almost) the same periodic porosity represented by the same Periodic Unit Cell (see Figure 2), since they differ only by a relative shift in their periodic micro-geometry, which can be described with parameter $\xi \in \langle 0, 1\rangle$ shown in Figure 2(middle). On the other hand, the relative shift in periodicity significantly affects the character of panel faces: one panel has uneven faces with small thin ribs separating circular indentations which gently lead the air to narrows slits (see the top sketch in Figure 1), while the other panel has flat faces with loosely spaced narrow slits (see the bottom sketch in Figure 1).

From the macroscopic perspective the material of both panels may be treated (after a homogenisation procedure) as the same porous medium, however, the surface effects may reveal at the macro-scale level, if the size of PUC is suitably large (as it is assumed in this study). The open porosity of the periodic material of both panels is composed of large cylindrical voids linked with narrow slits. The slits in the material are parallel to the direction of wave propagation, whereas the axes of cylindrical voids are perpendicular to this direction, so that the whole porous microstructure can be fully represented by the two-dimensional cross-sections shown in Figure 1; moreover, they can be used for efficient numerical analyses of the relevant microscopic problems.

The Periodic Unit Cell is depicted in Figure 2, where $L = 4\,\text{mm}$ is the cell size, $R = 1.6\,\text{mm}$ is the radius of all cylindrical voids, and $H = 0.4\,\text{mm}$ is the width of all slits. The panel is (in each case) composed of 15 full periodic cells, so its thickness is $\ell_p = 15L =$

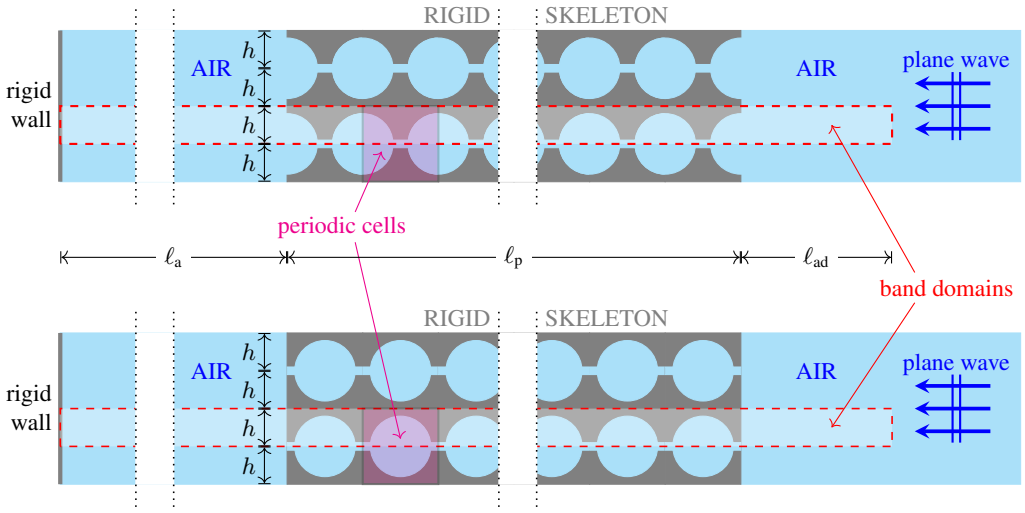

Figure 1: Porous panel backed with an air cavity – two studied cases based on the same periodic pattern of porosity, but with extremely different types of openings on the panel faces, related to a translation of the Periodic Unit Cell: (top) the panel with uneven faces (i.e., with densely spaced semi-circular indentations separated by ribs), and (bottom) the panel with flat faces with narrow slits

60 mm. The air cavity depth is $\ell_p = 20$ mm, and the included thickness of the adjacent air in front of the panel is $\ell_{ad} = 3L = 12$ mm. (It was checked that the adjacent layer – where the propagation is lossless – could be thinner and the numerical predictions of sound absorption would be the same anyway.)

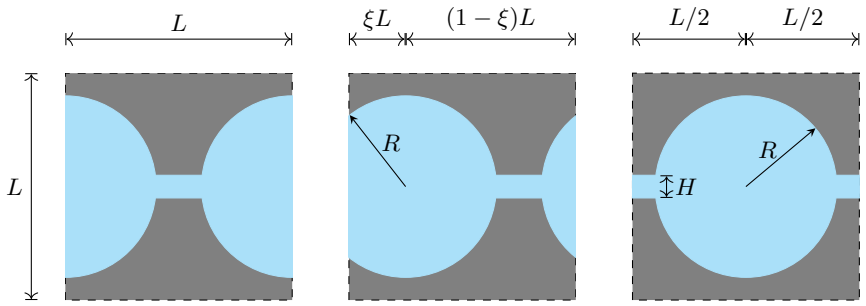

Figure 2: Two-dimensional Periodic Unit Cell with the open porosity composed of large cylindrical voids linked with narrow slits – three cases of translational symmetry resulting in different sizes of openings on the lateral faces of the cells

2.2. Porous samples with periodic microstructure

Two three-dimensional CAD models of cylindrical specimens were generated from the two-dimensional Periodic Unit Cell, see Figure 3(left). Small thin rings were added on the circumference of each cylinder to keep the solid parts of each specimen together.

The CAD models were used with Fused Deposition Modelling (FDM) technology of additive manufacturing [1] to fabricate polymer porous samples (each one with the diameter of 29 mm and the height of 60 mm), see Figure 3(right). As a matter of fact, these samples are cylindrical segments of porous panels which can be tightly fitted into the impedance tube for measurements of sound absorption.

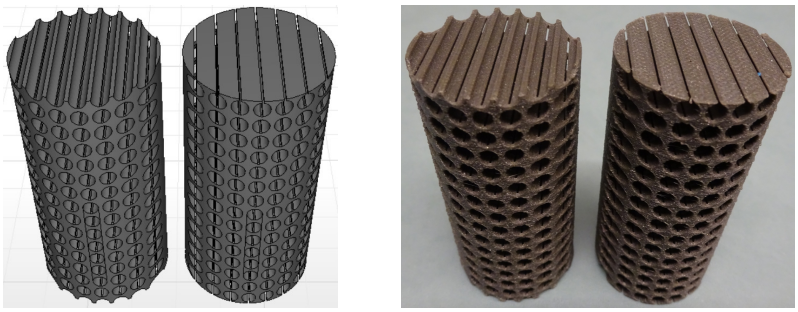

Figure 3: (Left) CAD models of cylindrical samples for the two cases of porous panel. (Right) two cylindrical samples fabricated using FDM technology

The samples were examined under a microscope to find that the actual size of cylindrical voids is significantly smaller. The corrected value for the cylindrical void radius was found as $\tilde{R} = 1.4\,\text{mm}$.

3. MODELLING

3.1. Direct Numerical Simulations (DNS)

The sound absorption of rigid periodic porous panels backed by air cavity (see Figure 1) can be determined numerically using Direct Numerical Simulations (DNS) based on the linearised Navier-Stokes equations transformed into the frequency domain. The equations describe the harmonic motion in a representative band of fluid domain, that is, in viscous and compressible air which fills the pores and slits, as well as the backing cavity, caused by a plane acoustic wave simulated by applying an adiabatic pressure excitation on a boundary situated at some (sufficiently large) distance ℓ_{ad} from the panel, so that also this adjacent layer of air in the front of panel is considered in the analysis. Thus, the total length of the band of air domain equals $\ell_{\text{a}} + \ell_{\text{p}} + \ell_{\text{ad}}$, and because of the symmetry its height is $h = L/2$, i.e., half the height of the periodic cell.

The symmetry conditions are set on the lateral boundaries of the representative band of fluid domain, and the isothermal no-slip boundary conditions are applied on the solid boundaries (that is, inside the pores and slits, on the panels' faces, and on the backing

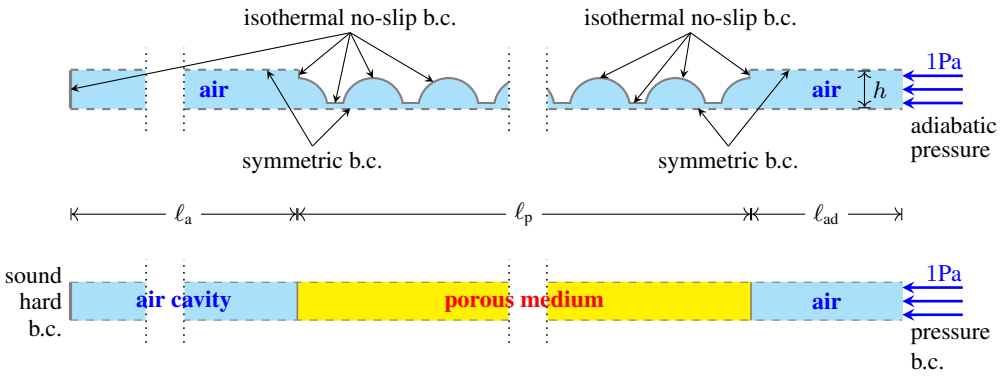

Figure 4: Computational configurations for periodically porous panel with "gaping" faces (i.e., the ribbed-faces case) and backed with air cavity: (top) for DNS using the linearised Navier-Stokes equations, and (bottom) for calculations using the Helmholtz equation for the air cavity and the homogenized JCAPL model of the porous layer

wall), see top sketches in Figures 4 and 5. In order to determine the sound absorption (which results from the boundary effects on the skeleton of porous panel and in the cavity), the surface acoustic impedance is computed on the 'adiabatic pressure boundary' as the negative ratio of the pressure to the normal velocity. This surface impedance together with the characteristic impedance of air allows to calculate the acoustic absorption coefficient in the considered frequency range.

3.2. Equivalent fluid approach

The solid skeleton of panel is rigid and motionless, therefore, the periodic porous layer of panel can be substituted with an equivalent layer of an effective (lossy and dispersive) fluid. Thus, the whole problem of acoustic plane wave propagation through the panel into the cavity and back (after the reflection from the rigid wall) can be solved on the macro-scale level using the Helmholtz equation of linear acoustics set in the cavity, in the effective-fluid domain of porous medium, and in the adjacent (frontal) air layer, see the bottom sketch in Figure 4. (The wave propagation in front of the panel is lossless, so the adjacent air layer could be removed, however, it is kept in these analyses for the sake of complete resemblance to the corresponding configurations of DNS.)

The equivalent acoustic fluid is characterised by the frequency-dependent effective density and bulk modulus, namely:

$$\varrho_{\text{eff}}(\omega) = \frac{\varrho_{\text{air}}\,\alpha(\omega)}{\phi}\,, \qquad K_{\text{eff}}(\omega) = \frac{K_{\text{air}}}{\phi\left[\gamma - (\gamma-1)/\alpha'(\omega)\right]}\,, \tag{1}$$

where ω is the angular frequency, ϕ is the (open) porosity, ϱ_{air} and K_{air} are the density and bulk modulus of air which fills the pores, respectively, and γ is the ratio of specific heats for air; finally $\alpha(\omega)$ and $\alpha'(\omega)$ are two complex-valued functions of dynamic tortuosity: the viscous and thermal one, respectively. According to the Johnson-Champoux-Allard-Pride-Lafarge (JCAPL) model [5, 16–20] these two functions depend of the kinematic viscosity of air and its Prandtl number, as well as on the eight transport parameters, namely: the porosity ϕ, the (inertial) tortuosity α_∞, the static viscous and thermal tortuosities α_0 and α_0', the viscous and thermal permeabilities k_0 and k_0', and the viscous and thermal characteristic lengths Λ and Λ'. The parameters can be determined for any Periodic Unit Cell: the porosity and thermal length are derived directly from its geometry, while the other parameters require solutions of three uncoupled problems of Stokes, Laplace, and Poisson, respectively, defined on the fluid domain of PUC, see e.g., [7, 8, 11]. For the considered PUC (see Figure 2) with the actual value of the cylindrical pore radius $R = \tilde{R} = 1.4\,\text{mm}$, the transport parameters were determined as follows: $\phi = 41.5\%$, $\alpha_\infty = 2.15$, $\alpha_0 = 2.67$, $\alpha_0' = 1.41$, $k_0 = 3.43\times10^{-9}\text{m}^2$, $k_0' = 9.67\times10^{-8}\text{m}^2$, $\Lambda = 0.475\,\text{mm}$, $\Lambda' = 1.27\,\text{mm}$.

The Helmholtz problem is solved for the macro-scale configuration shown in Figure 4(bottom) with the sound hard boundary condition on the left-hand side boundary (i.e, on the rigid wall), the acoustic pressure condition on the right-hand side boundary, and coupling on the interfaces between the adjacent media. This is, in fact, a one-dimensional problem of plane wave propagation, so it renders a system of ordinary-differential equations, which can be solved analytically. When the solution is found, the surface acoustic impedance is computed on the right-hand side boundary and the acoustic absorption coefficient can be determined for such configuration of the porous layer (panel) backed with air cavity.

3.3. Sandwich porous layer with thin face-layers of modified tortuosity

The results of the DNS and Helmholtz (JCAPL-based) calculations will be compared in Section 4 to show, in fact, a very good consistence. Direct Numerical Simulations were also carried out for the second version of porous panel, that is, the one with the same thickness and periodic porosity in general, but with the flat slotted faces (because of a simple shift in periodicity), as presented in Figure 5(top). It will be demonstrated that the sound absorption computed from DNS for this panel (set in the same macro-scale configuration as the other version) differs from the results obtained for the first version of panel by a small shift in frequency. It is expected that this inaccuracy arises from the distortion of the air flow induced by the flat surfaces between the narrow slits. It causes additional viscous effects at the panel faces around the slits where the flow bends around.

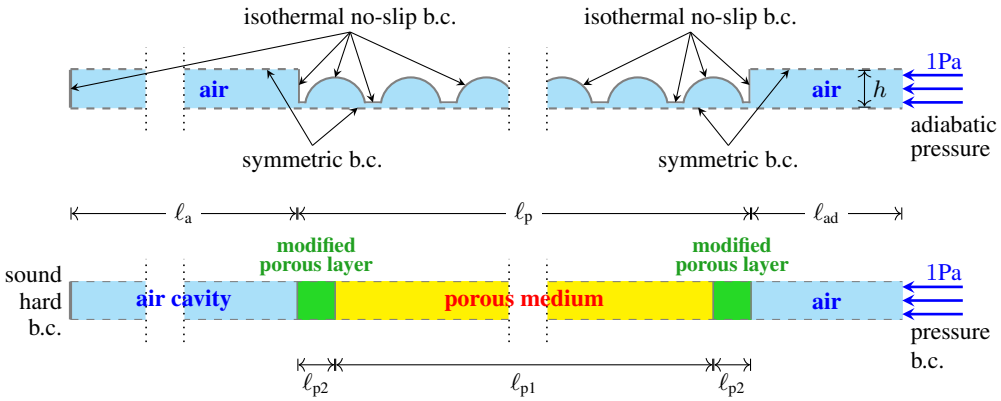

Figure 5: Computational configurations for periodically perforated panel with flat slotted faces (i.e., the slotted-surface case) and backed with air cavity: (top) for DNS using the linearised Navier-Stokes equations, and (bottom) for calculations using the Helmholtz equation for the air cavity and the homogenized JCAPL models of three porous layers in a sandwiched arrangement

It is obvious that the transport parameters for the second version of panel are the same as for the first version, since their periodic porosity is defined by the same PUC, and the periodic Stokes, Laplace, and Poisson problems will have (respectively) exactly the same solutions for any PUC version shown in Figure 2 (and for any relative shift $\xi \in \langle 0, 1 \rangle$). Therefore, in order to account for the flow distortion at the flat faces of panel, a special correction must be applied in the macro-scale modelling based on the JCAPL model of effective fluid. Following the approach used in the case of thin micro-perforated plates.

A sandwich configuration is proposed (see the bottom sketch in Figure 5) with: (1) the core of the effective medium exactly the same as in the layer used as substitute for the first version of panel (see Section 3.2), and (2) the thin face-layers of a similar porous material as the core, but with modified tortuosity. The thickness of each face layer is assumed equal to the half size of PUC, namely, $\ell_{p2} = 0.5L = 2\,\text{mm}$, so that the core layer has the same faces as in the first version of panel and the core layer thickness is $\ell_{p1} = \ell_p - 2\ell_{p2} = 14L = 56\,\text{mm}$, see Figure 5(bottom). The (inertial) tortuosity and viscous static tortusoities for the porous face-layers are (arbitrarily) increased by 35% with respect to the tortuosity values of the core layer, namely, $\tilde{\alpha}_\infty = c_\alpha\,\alpha_\infty$ and $\tilde{\alpha}_0 = c_\alpha\,\alpha_0$, where $c_\alpha = 1.35$ is the correction coefficient (the same for both tortuosities). All the other transport parameters are the same for the face- and core layers.

4. SOUND ABSORPTION

4.1. Numerical predictions

Figure 6 presents numerical predictions of sound absorption for the both cases of porous panel backed with air cavity. DNS results for the case with ribbed "gaping" faces is very similar to the Helmoltz results where the panel was modelled as a single layer of homogeneous porous medium using JCAPL model (with transport parameters computed from PUC). DNS results for the panel with flat slotted faces show that the absorption peaks are slightly shifted down in frequency (by several dozens or a few hundreds of hertz). It is assumed that this effect results from the distortion of the air flow at the panel flat faces with narrow loosely set slits. In Section 3.3 it has been proposed that in order to account for this effect in the macro-scale modelling (where the JCAPL model of the effective medium equivalent to a porous material is used), the tortuosity of the porous material should be increased, but only for the area close to the panel faces, which is achieved by introducing a sandwiched arrangement of porous media. This simple correction allowed to fit the sound absorption obtained from the macro-scale Helmholtz calculations for the porous sandwich layer with the direct micro-scale simulation for the panel microstructure with flat slotted faces, see Figure 6.

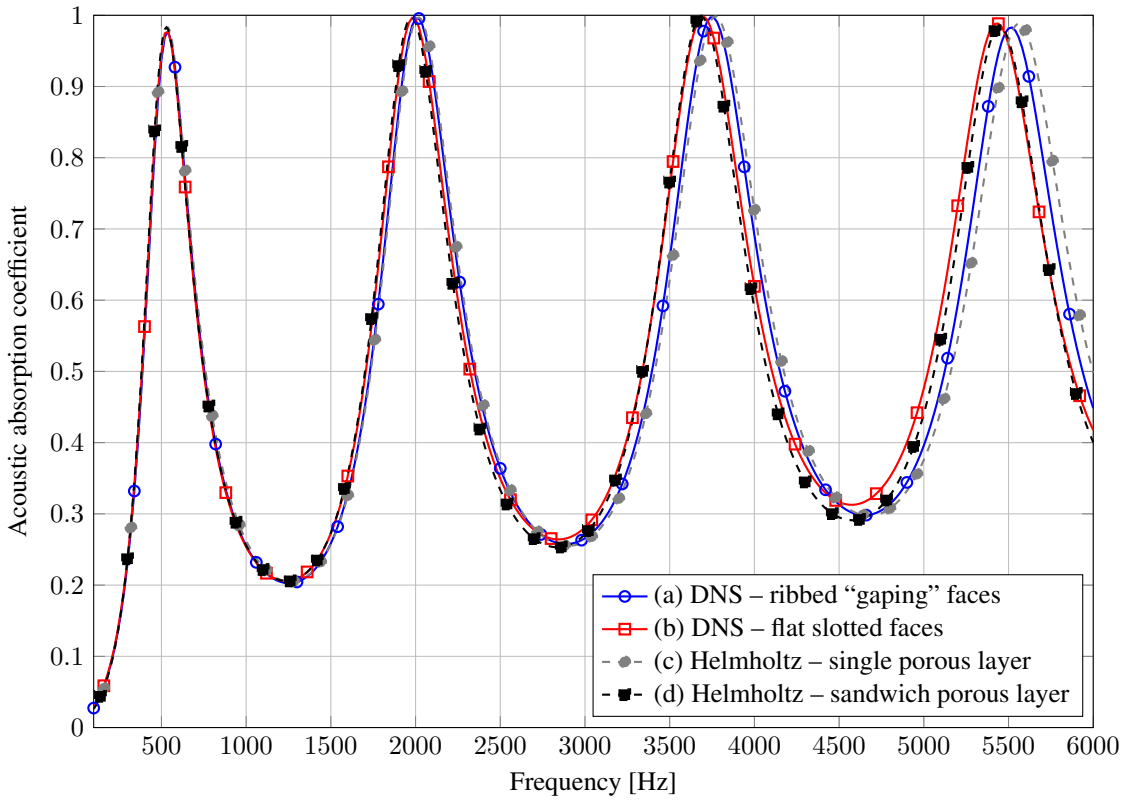

Figure 6: Sound absorption for porous panels backed with air cavity: (a,c) the DNS and Helmholtz (with a single JCAPL layer) for the ribbed "gaping" faces case, (b,d) the DNS and Helmholtz (with three JCAPL layers in sandwiched arrangement) for the slotted faces case

4.2. Experimental measurements

Sound absorption was measured in the impedance tube for both 3D-printed polymer samples (60 mm in height) with a 20 mm cavity between the back face of the sample and the rigid termination of the tube. The measurements are shown in Figure 7 where they are compared with the results of numerical predictions by DNS. The same shift in frequency of the absorption peaks between the flat slotted faces case and the ribbed "gaping" faces case is observed experimentally as it has been found by the numerical predictions. On the other hand, between the peaks the measured absorption values are clearly higher than the predictions. However, this underestimation was expected since idealised *smooth* micro-geometries were used for the microstructure-based calculations (DNS and PUC-based), while the actual microstructures of the 3D-printed samples are characterised by many imperfections (like roughness, small fibres etc.) which are expected to increase, in general, the viscous dissipation effects.

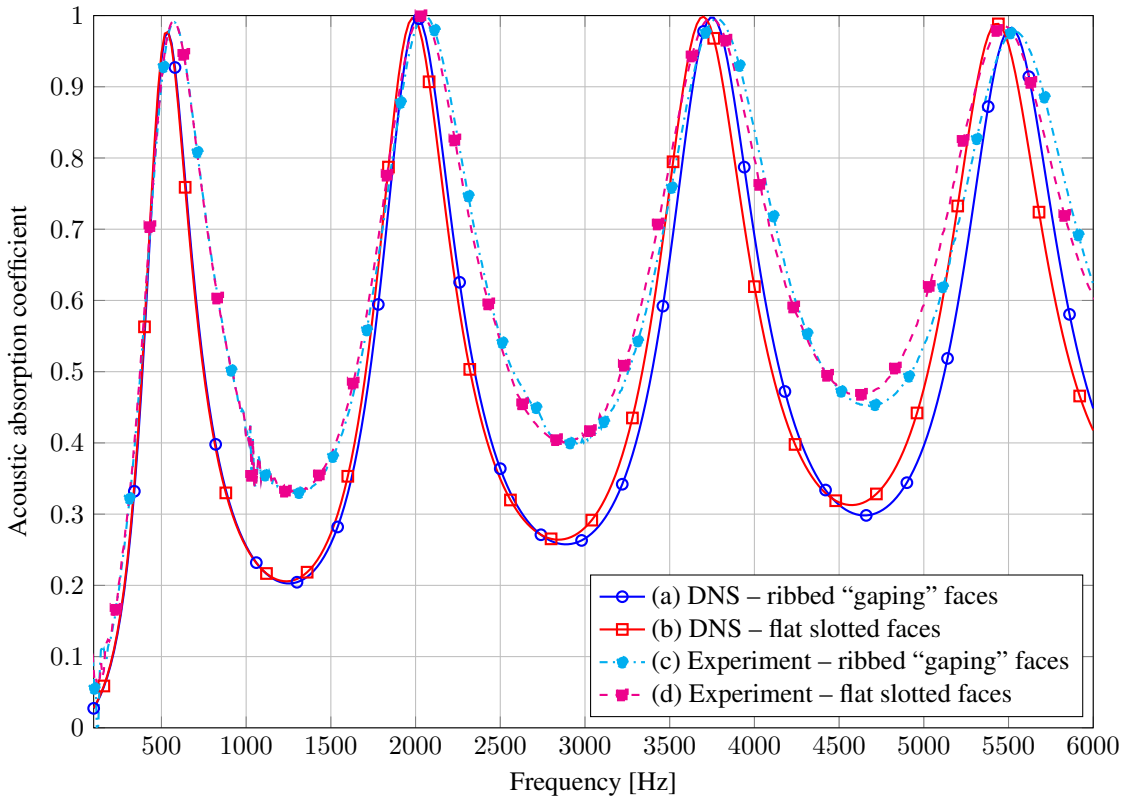

Figure 7: Sound absorption for porous panels backed with air cavity: (a,c) the DNS results and measurements for the ribbed "gaping" faces case, (b,d) the DNS results and measurements for the case of slotted faces

5. CONCLUSIONS

Samples fabricated using modern manufacturing technologies and CAD models of designed microstructures require a special microscopic survey in order to update their CAD geometry, if it is to be used for microstructure-based calculations; alternatively, these CAD models should be appropriately modified before being used for manufacturing. Otherwise, significant discrepancies will arise between the measurements of acoustic

absorption and the corresponding results of modelling, perhaps even in the very nature of the absorption curves (e.g., peaks at quite different frequencies, etc.). The updating of CAD geometry can be often done in a simple way (since the geometry was designed), however, even then, the absorption predictions, though completely correct in character, will almost always give slightly underestimated values due to imperfections in the surface (e.g., roughness) caused by manufacturing technologies.

The effect of a relative shift in periodicity demonstrated in this work was observed experimentally for various 3D-printed samples based on the same periodic cell. It was confirmed that the associated shift in the frequency, although small, is not casual and is related to a different flow distortion at the faces of the material samples.

6. ACKNOWLEDGEMENTS

This research collaboration is supported by COST (European Cooperation in Science and Technology) through the COST Action CA15125 – DENORMS: "*Designs for Noise Reducing Materials and Structures*". T. G. Zieliński would like to acknowledge the financial support of the Project "*Relations between the micro-geometry and sound propagation and absorption in porous and poroelastic media*", No. 2015/19/B/ST8/03979, financed by the Polish National Science Centre (NCN). M. Červenka would like to acknowledge the financial support by GACR grant GA18-24954S.

7. REFERENCES

[1] T. D. Ngo, A. Kashani, G. Imbalzano, K. T. Nguyen, and D. Hui. Additive manufacturing (3D printing): A review of materials, methods, applications and challenges. *Composites Part B*, 143:172–196, 2018.

[2] T. G. Zieliński. Pore-size effects in sound absorbing foams with periodic microstructure: modelling and experimental verification using 3D printed specimens. In P. Sas, D. Moens, and A. van de Walle, editors, *Proceedings of ISMA2016 International Conference on Noise and Vibration Engineering and USD2016 International Conference on Uncertainty in Structural Dynamics*, pages 95–104, 2016.

[3] T. G. Zieliński, F. Chevillotte, and E. Deckers. Sound absorption of plates with micro-slits backed with air cavities: Analytical estimations, numerical calculations and experimental validations. *Applied Acoustics*, 146:261–279, 2019.

[4] ISO 10534-2: Determination of sound absorption coefficient and impedance in impedance tubes, 1998.

[5] J. F. Allard and N. Atalla. *Propagation of Sound in Porous Media: Modelling Sound Absorbing Materials, Second Edition*. Wiley, 2009.

[6] S. Gasser, F. Paun, and Y. Bréchet. Absorptive properties of rigid porous media: Application to face centered cubic sphere packing. *J. Acoust. Soc. Am.*, 117(4):2090–2099, April 2005.

[7] C. Perrot, R. Panneton, and X. Olny. Periodic unit cell reconstruction of porous media: Application to open-cell aluminum foams. *J. Appl. Phys.*, 101:113538, 2007.

[8] C.-Y. Lee, M. J. Leamy, and J. H. Nadler. Acoustic absorption calculation in irreducible porous media: A unified computational approach. *J. Acoust. Soc. Am.*, 126(4):1862–1870, October 2009.

[9] F. Chevillotte, C. Perrot, and R. Panneton. Microstructure based model for sound absorption predictions of perforated closed-cell metallic foams. *J. Acoust. Soc. Am.*, 128(4):1766–1776, October 2010.

[10] C. Perrot, F. Chevillotte, M. T. Hoang, G. Bonnet, F.-X. Bécot, L. Gautron, and A. Duval. Microstructure, transport, and acoustic properties of open-cell foam samples: Experiments and three-dimensional numerical simulations. *J. Appl. Phys.*, 111:014911, 2012.

[11] T. G. Zieliński. Microstructure-based calculations and experimental results for sound absorbing porous layers of randomly packed rigid spherical beads. *J. Appl. Phys.*, 116:034905, 2014.

[12] T. G. Zieliński. Generation of random microstructures and prediction of sound velocity and absorption for open foams with spherical pores. *J. Acoust. Soc. Am.*, 137:1790–1801, 2015.

[13] X. H. Yang, S. W. Ren, W. B. Wang, X. Liu, F. X. Xin, and T. J. Lu. A simplistic unit cell model for sound absorption of cellular foams with fully/semi-open cells. *Compos. Sci. Technol.*, 118:276–283, 2015.

[14] T. G. Zieliński. Microstructure representations for sound absorbing fibrous media: 3D and 2D multiscale modelling and experiments. *J. Sound Vib.*, 409:112–130, 2017.

[15] J. H. Park, K. S. Minn, H. R. Lee, S. H. Yang, C. B. Yu, S. Y. Pak, C. S. Oh, Y. S. Song, Y. J. Kang, and J. R. Youn. Cell openness manipulation of low density polyurethane foam for efficient sound absorption. *J. Sound Vib.*, 406:224–236, 2017.

[16] D. L. Johnson, J. Koplik, and R. Dashen. Theory of dynamic permeability and tortuosity in fluid-saturated porous media. *J. Fluid Mech.*, 176:379–402, 1987.

[17] Y. Champoux and J.-F. Allard. Dynamic tortuosity and bulk modulus in air-saturated porous media. *J. Appl. Phys.*, 70:1975–1979, 1991.

[18] S. R. Pride, A. F. Gangi, and F. D. Morgan. Deriving the equations of motion for porous isotropic media. *J. Acoust. Soc. Am.*, 92(6):3278–3290, 1992.

[19] S. R. Pride, F. D. Morgan, and A. F. Gangi. Drag forces of porous-medium acoustics. *Phys. Rev. B*, 47(9):4964–4978, 1993.

[20] D. Lafarge, P. Lemarinier, J. F. Allard, and V. Tarnow. Dynamic compressibility of air in porous structures at audible frequencies. *J. Acoust. Soc. Am.*, 102(4):1995–2006, 1997.